

NAVIER-STOKES ANALYSIS OF GA(W)-2 AEROFOIL WITH DEFLECTED FLAP AND REDESIGN OF HANSA FLAP FOR BETTER PERFORMANCE

S. K. CHAKRABARTTY[‡]K. DHANALAKSHMI[†]V. RAMESH[†]

Abstract

Navier-Stokes analysis of flow past GA(W)-2 aerofoil with deflected flap is presented in this paper. Extensive computations have been carried out for various flap deflections using JUMBO2D code. JUMBO2D is a two-dimensional analysis code, which solves compressible Reynolds Averaged Navier Stokes (RANS) equations using a vertex based finite volume space discretization, five-stage Runge-Kutta time integration and algebraic turbulence model. All the results have been validated by comparing with experimental values. Inter-code comparison has also been done for some specific cases.

Design-analysis studies of an aerofoil-flap configuration proposed to be used in a low speed aircraft HANSA 3, designed, developed and built by NAL, Bangalore is also reported in this paper. This part of the work is in continuation of the effort reported earlier on redesign of HANSA-3 flap using CFD where the changes were proposed at the trailing edge region of the main aerofoil and on the leading edge of the flap. Implementation of those changes became difficult as this would mean modifying the trailing edge spar located in this region. Therefore, an effort has been made here to re-design the aerofoil flap configuration without affecting the main aerofoil upto the trailing edge spar.

Key Words: Control surface design, Aerofoil, flap, Navier-Stokes equations, Attached and separated flows

1 Introduction

Computational Fluid Dynamics can play an important role in design, development and analysis of an aircraft and its components for better performance. It is essential to solve Reynolds Averaged Navier-Stokes (RANS) equations, with a suitable turbulence model, to obtain detailed analysis of the flow parameters particularly the boundary-layer and flow separation. The study of two dimensional viscous flow past multi-element aerofoils or aerofoils with deflected flaps, prediction of $C_{l,max}$ and the post stall behaviour of the aerofoil need a very accurate RANS solver with rea-

sonably good and robust turbulence model. Many numerical schemes have now been developed which can accurately compute viscous flows in complex regions. These schemes require a computational grid capable of resolving all the flow features of interest. The geometry of aerofoil with flap is such that a single-block structured grid is not suitable and either unstructured grid or a multi-block structured grid is necessary. A two-block grid, suitably clustered and near-orthogonal at the aerofoil surfaces in order to get an accurate resolution of the boundary layer, has been generated here using GRIDGEN [1] code. The JUMBO2D computer code solves the two-dimensional RANS equations using a vertex based finite volume space discretization, and five-stage Runge-Kutta time integration. Local time stepping and implicit residual smoothing are used for convergence acceleration. An algebraic turbulence model is used for the computation of turbulent flows. Details of the governing equations, boundary conditions, finite volume space discretisation, time integration and the turbulence model used are available in [2, 3, 4, 5, 6, 7]. The code is independent of the grid

Received on March 17, 2003.

[†] Computational and Theoretical Fluid Dynamics
Division, National Aerospace Laboratories;
Bangalore 560 017, India

[‡] drske@cfdl.cnmr.ernet.in

topology used, and the only necessary input is the grid data. The computational domain can be subdivided into smaller subdomains/blocks and the computation can be carried out blockwise to reduce the memory requirement and to facilitate parallel computation. The blocks are connected by overlapping one or two layers of grid cells, and the boundary data are transferred by using, in the input data, an apriori specification of the proper block connections. The type of the boundary conditions to be specified at each segment of a face of a particular block can be specified through input data. These make the code very flexible, and allow the same code to solve a variety of flow problems including internal flows [2, 5, 8]. A novel space discretization scheme is used here for the viscous terms, which facilitates computation of full Navier-Stokes equations with about the same numerical effort as for the thin layer type of approximation [3]. The algebraic turbulence model of Baldwin-Lomax [6, 7] has been used here assuming that the flow is fully turbulent.

In the present study the aerofoil configuration with flap has been considered. The gap between the main aerofoil and the flap has been simulated by a separate block of grid with two opposite faces representing the trailing edge part of the main aerofoil (cove region) and the leading edge part of the flap. The other two faces connect the surrounding C-type grid. The flow is assumed to be fully turbulent everywhere except in this small gap, where it is assumed to be laminar.

RANS computations for a single GA(W)-2 aerofoil upto and beyond stall have been performed by Vimala[9]. However, these results are for only single element aerofoil and this can be considered to be equivalent to zero flap deflection. We have further computed for the cases of flap deflection angles of $\delta = 10^\circ$ and $\delta = 20^\circ$. These results are compared with the experimental results [10, 11] and for $\delta = 0^\circ$ case, with [9] also. The purpose of this exercise of RANS computation for flap deflected configuration was to demonstrate the capability of JUMBO2D code for predicting the aerodynamic characteristics for the complete range of angles of attack including post stall. This also gives us more confidence in the redesign work of the HANSA-3 flap configuration where there are no experimental results to compare. HANSA-3 is a two seater, all composite trainer aircraft designed and developed at NAL, India.

The earlier work on redesign of HANSA-3 flap[12, 13] involved major modifications of profiles of both the flap and main aerofoil. However the implementation of the modified profile for the main aerofoil could not be carried out. This is because the trailing edge spar located at the flap cove region could not be disturbed as required by the modified profile of the main aerofoil.

Hence there was a need to reconsider the design work, such that a new configuration could be arrived at without disturbing the flap cove region of the main aerofoil. With this new constraint we have now arrived at a new design which is mainly concerned with the design of the flap profile and some minor modification to the cove region which does not disturb the existing trailing edge spar.

2 Results and Discussion

2.1 Validation of JUMBO2D for GA(W)-2 aerofoil with flap

Two block grids have been generated for computations of flow past GA(W)-2 aerofoil. The outer block is C-Type with (392 x 62) points and the inner block, which fills the gap region, is H-type with (32 x 63) points. Only the C-type outerblock grid is used for $\delta = 0^\circ$ case. Out of the 392 points in i-direction, first and last 45 points are in the wake region. The normal distance of the first grid line from the aerofoil surface is approximately (0.5×10^{-4}) . This gives an average law-of-the-wall coordinate, $Y^+ = 4$ at the first node point. Leading edge of the main aerofoil is situated at the origin. Reference length scale is the chord length defined as the distance from the origin to the trailing edge of the flap at zero degree deflection. The chord is of unit length and lies on the x-axis, while the y-axis is normal to it. Far field boundary of the outer block extends from 9-chords upstream to 11-chords downstream. In the normal direction the outer boundary extends upto 10-chords. The extent of computational outer boundary has been finalised after a careful study such that further extension does not have any significant effect on the solution. A typical view of the grids for all the three cases of flap deflection $\delta = 0^\circ, 5 = 10^\circ$ and $\delta = 20^\circ$ are shown in Fig.1(a), (b) and (c) respectively. All the computations have been done for free-stream Mach number, $M_\infty = 0.13$, and $Re_\infty = 2.2 \times 10^6$ to compare with available experimental results [10, 11]. Tables 1, 2 and 3 give the various computed coefficients for the three cases of flap deflection.

Figure 2(a) shows the comparison of computed lift coefficient with the experimental values for various angles of attack for all the three flap deflections. It can be seen from the figure that except in the region close to the stall, the code predicts lift coefficient, C_L very well for the complete range of α 's. Also in the attached regions of the flow a complete linear behaviour of the lift curve is satisfactorily predicted. It can be observed from the tables and figures for $\delta = 0^\circ, \delta = 10^\circ$ and $\delta = 20^\circ$ that the code predicts stall at $16^\circ, 16^\circ$ and 14° respectively. This is in good agreement with the experimental values. Figure 2(b) shows the comparison of the drag coefficient C_D . An overall good agreement

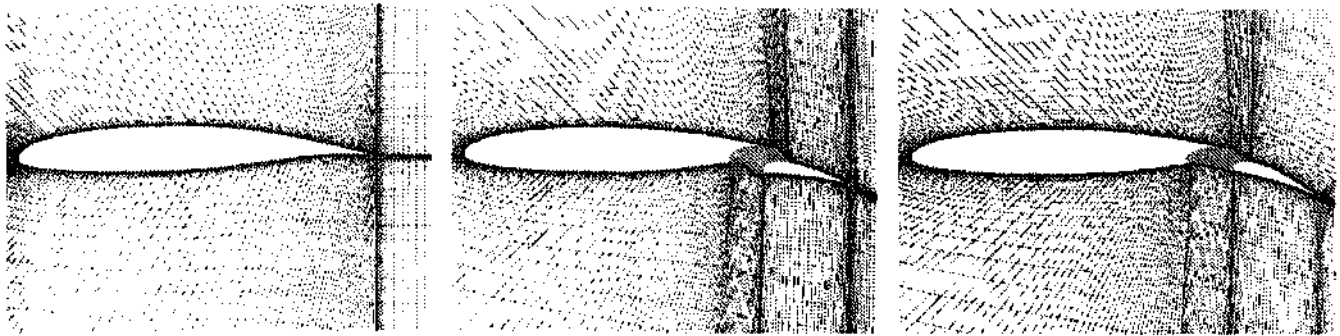
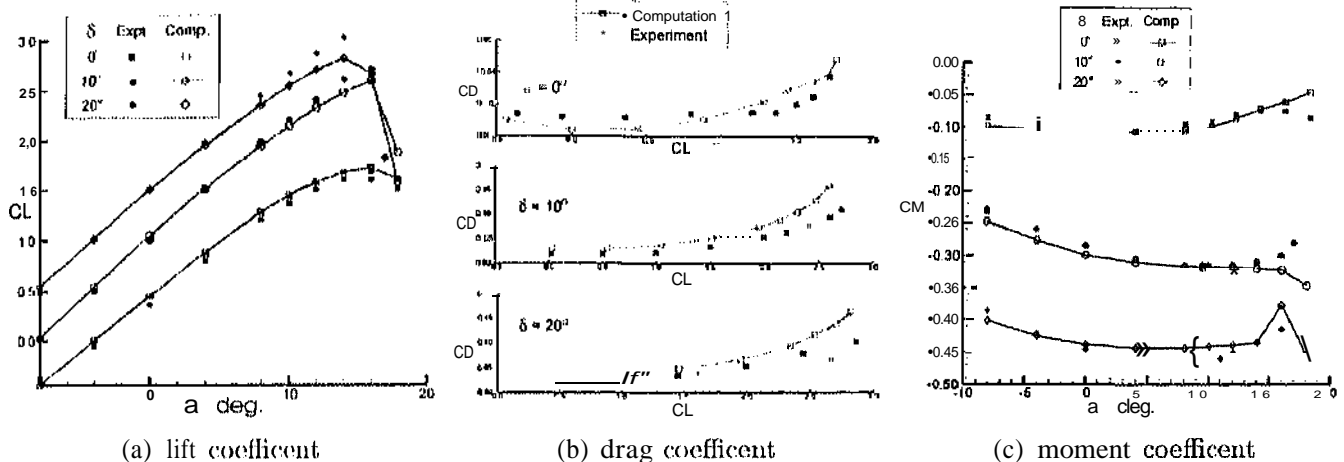
(a) $\delta = 0^\circ$ (b) $\delta = 10^\circ$ (c) $\delta = 20^\circ$

Fig.1: A Partial View of the grid for GA(W)-2 aerofoil



(a) lift coefficient

(b) drag coefficient

(c) moment coefficient

Fig.2: Comparison of aerodynamic coefficients for GA(W)-2 aerofoil with flap:

$$M_\infty = 0.13, Re_\infty = 2.2 \times 10^6$$

can be observed except at higher values of C_L , where the present computation slightly over predicts the C_D values. A very much similar comparison can be seen for the moment coefficient, C_m in Fig.2(c). Again, in this case a slight deviation from the experiment is seen for higher values of α close to the stall.

Fig.3(a) shows a comparison of computed pressure coefficient, C_p , with two experimental results of NASA[10] and WSU[11] and also with computed results of Vimala[9] for three angles of attack, $\alpha = 0^\circ, 8^\circ$, and 16° with flap deflection angle set at $\delta = 0^\circ$. Here, the results of [9] are for $M_\infty = 0.3$, and the comparison is very good except near the leading edge. Similarly, for $\delta = 10^\circ$, Fig.3(b) shows the comparison of pressure coefficient for $\alpha = 0^\circ, 8^\circ$, and 10° and Fig.3(c) shows the same for $\delta = 20^\circ$ and $\alpha = 0^\circ, 8^\circ$ and 14° . It can be observed from all these figures, that very good comparisons have been obtained with the experimental values. In Fig.3(b), however, the discrepancies are observed particularly near the leading edge of the flap. This is because the flow in this region is through a constricted narrow gap between the lower portion of the

main aerofoil trailing edge and the upper portion of the leading edge of the flap. However for $\delta = 20^\circ$, a better comparison is obtained even in this region because in this case, the width of the gap between the main aerofoil and the flap is increased with higher angle of flap deflection.

Figure 4(a) and (b) shows streamline pattern superimposed on Mach contours for $\alpha = 0^\circ$ and $\alpha = 8^\circ$ respectively for various flap deflections. It can be clearly observed that a very smooth flow pattern has been predicted. Fig.4(c) shows a similar plot for $\alpha = 16^\circ$. This is the case of high angle of attack, around stall. In this case we notice that the flow is attached for $\delta = 10^\circ$ and for $S = 0^\circ$ and $S = 20^\circ$ a tendency of the flow to separate. This can be attributed to the presence of small vortex structures near the trailing edges. Finally Fig.4(d) shows streamline pattern superimposed on Mach contours for post stall cases for $\alpha = 0^\circ, 10^\circ$ and 20° wherein one can see large regions of separated flow with vortex structures on the flow downstream of the trailing edge of the main aerofoil.

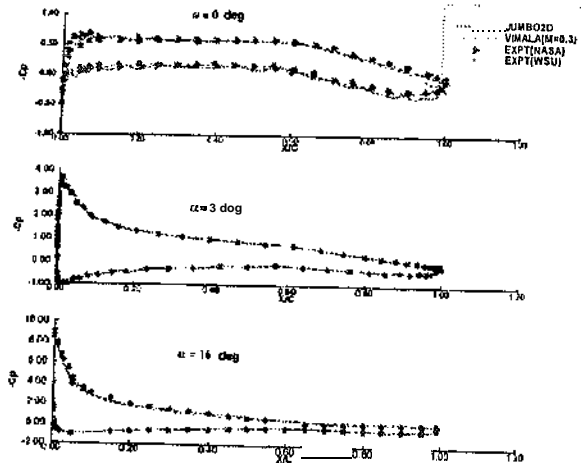
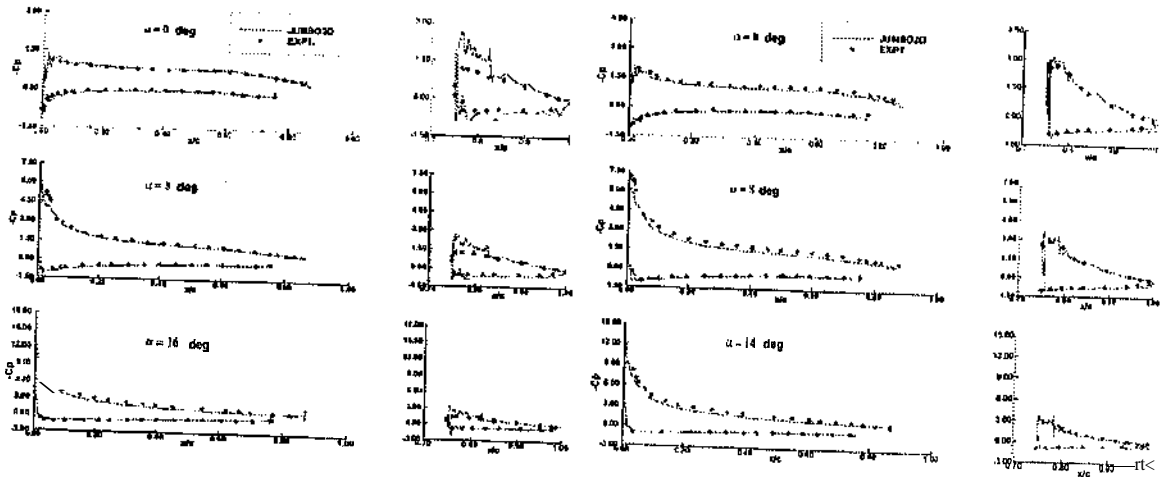
(a) $\delta = 0^\circ$ (b) $\delta = 5^\circ$ (c) $\delta = 20^\circ$

Fig.3: Comparison of pressure coefficient for GA(W)-2 aerofoil with flap:
 $M_\infty = 0.13$, $Re_\infty = 2.2 \times 10^6$

It is to be noted that the present code is capable of doing an accurate analysis for all the cases considered here. From these various comparisons of results with experiment for the GA(W)-2 case, it is felt that the JUMBO2D code has been very well validated for the analysis of the aerofoil with deflected flap. After this validation exercise, the same code is used for the analysis and design of the HANSA-3 aerofoil with flap.

3 Design and Analysis of HANSA-3 Aerofoil with Flap

Modified profiles of the aerofoil and flap for HANSA-3 aircraft were reported earlier in [12, 13] after a series of design and analysis work carried out using JUMBO2D code. These modified profiles showed a significant improvement in the flow behaviour at higher α 's for all flap deflected cases considered there. However, that

α	C_L	C_D	C_M	C_{Df}
-8.00	-0.433779	0.010101	-0.098064	0.63885E-02
-4.00	0.002861	0.00388G	-0.102831	0.62856E-02
0.00	0.450838	0.004760	-0.106488	0.63308E-02
4.00	0.880918	0.010410	-0.106055	0.64051E-02
8.00	1.274888	0.021848	-0.103763	0.63477E-02
10.00	1.444162	0.029182	-0.099225	0.62009E-02
12.00	1.574863	0.034532	-0.085893	0.60214E-02
14.00	1.672405	0.039638	-0.071838	0.58243E-02
16.00	1.720114	0.048396	-0.061144	0.55977E-02
18.00	1.603768	0.075952	-0.046923	0.45922E-02

Table 1: GA(W)-2 : Aerodynamic coefficients for different α , $M_\infty = 0.13$, $\delta = 0^\circ$, $Re_\infty = 2.2 \times 10^6$

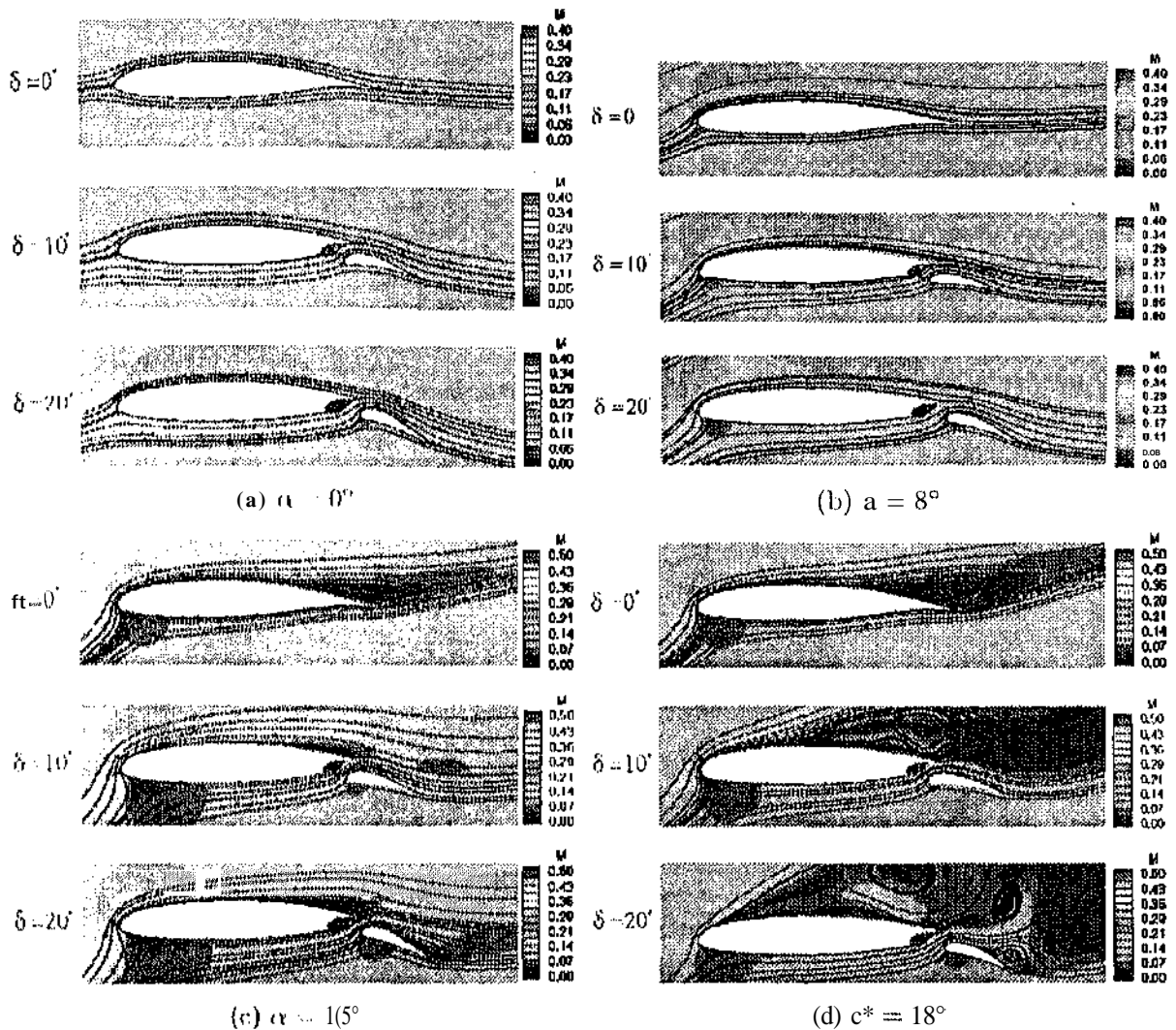


Fig.4: Streamlines and Mach contours for GA(W)-2 aerofoil with flap:

$$M_{\infty} = 0.13, Re_{\infty} = 2.2 \times 10^6$$

particular design could not be implemented because the modified profiles called for a lot of changes in the trailing edge portion of the main aerofoil which interfered with the spur located in this region. Therefore, in the present work we aim to redesign the profiles with minimum changes in the main aerofoil geometry. This has been achieved by incorporating small changes in the cove region, the flap geometry and the position of the point of rotation for the flap. After each change, viscous analysis was done and the changes in the flow pattern obtained was observed carefully to guide for further incremental changes. This iteration process was continued until the desirable flow pattern was achieved for all the three cases of deflected flap.

Figure 5¹ shows a comparison of the existing and

the present modified profiles of the main aerofoil and the flap. The co-ordinates of the point of rotation for the existing and the modified configuration are also given in Fig.5. Figure 6¹ shows the modified HANSA-3 aerofoil with the flap deflected at three angles corresponding to $\delta = 0^\circ, 10^\circ, 20^\circ$. The grid topology used for this case is exactly similar to that used for GA(W)-2 aerofoil. For all the cases two block grids have been used. Outer C-type block consists of (355 x 62), (375 x 62), (395 x 62) points and the inner block contains (12 x 63), (22 x 63), (32 x 62) points for ($\delta = 0^\circ, 10^\circ$ and 20° , respectively). For all the cases, in i direction, first and last 45 points are in the wake region.

Figure 7 shows typical views of the grids used for all the three flap positions. Figure 8(a) shows the variation of computed lift coefficient C_L with α for

¹Figures 5 and 6 are in page 96

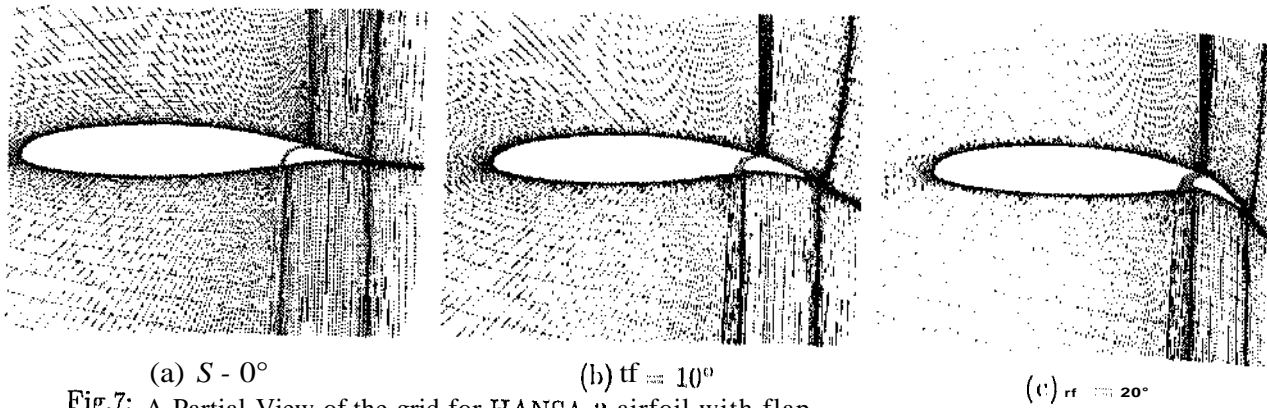
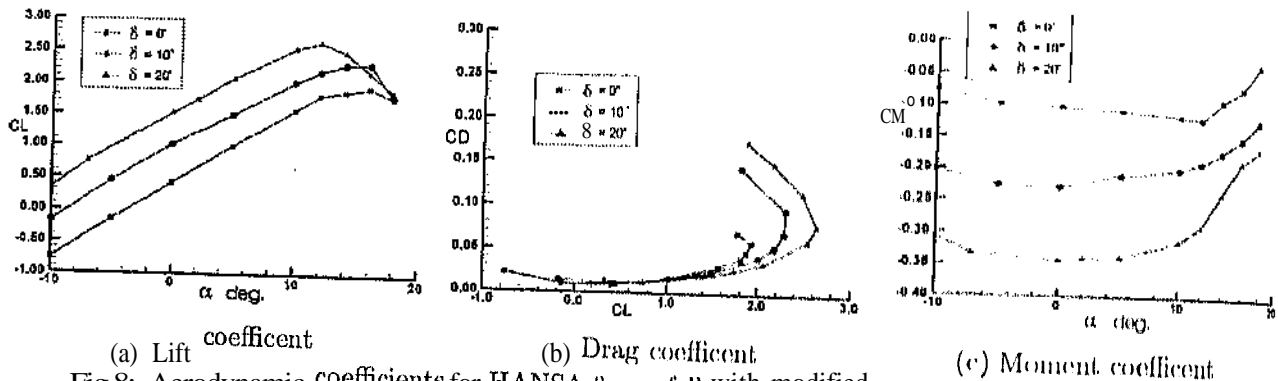


Fig.7: A Partial View of the grid for HANSA-3 airfoil with flap

Fig.8: Aerodynamic coefficients for HANSA-3 aerofoil with modified flap:
 $M_\infty = 0.3, Re_\infty = 2 \times 10^6$

α	C_L	C_D	C_M	C_{D_I}
-8.00	0.027247	0.030163	-0.247263	0.426451E-02
-4.00	0.543652	0.030316	-0.277514	0.428771E-02
0.00	1.049912	0.036999	-0.299806	0.430981E-02
4.00	1.513306	0.051429	-0.310542	0.4328110E-02
8.00	1.940063	0.073992	-0.316330	0.407961E-02
10.00	2.137473	0.088898	-0.317764	0.389481E-02
12.00	2.319097	0.105904	-0.316905	0.370831E-02
14.00	2.473727	0.130449	-0.320229	0.341361E-02
16.00	2.593397	0.159570	-0.321870	0.3140410E-02
18.00	1.879837	0.295421	-0.345393	0.154751E-02

Table 2: GA(W)-2 : Aerodynamic coefficients for different α , $M_\infty = 0.13, \delta = 10^\circ, Re_\infty = 2.2 \times 10^6$

α	C_L	C_D	C_M	C_{D_I}
-8.00	0.545231	0.032978	-0.400826	0.715621E-02
-4.00	1.020030	0.038060	-0.424293	0.708971E-02
0.00	1.506120	0.048201	-0.438144	0.724521E-02
4.00	1.941548	0.061542	-0.442983	0.711201E-02
8.00	2.341728	0.094700	-0.443150	0.662711E-02
10.00	2.538054	0.116245	-0.440994	0.637711E-02
12.00	2.698355	0.138612	-0.438876	0.611881E-02
14.00	2.810494	0.163764	-0.435082	0.565481E-02
16.00	2.657871	0.179408	-0.377316	0.278111E-02
18.00	1.572166	0.455029	-0.453696	0.294921E-02

Table 3: GA(W)-2 : Aerodynamic coefficients for different α , $M_\infty = 0.13, \delta = 20^\circ, t_{tr(H)} = 2.2 \times 10^6$

$\delta = 0^\circ, 10^\circ$ and 20° . An important feature that can be observed is that for all the flap deflections, the modified configuration shows almost a linear behaviour in the attached flow regions. With the increase in flap deflection angle the maximum C_L also increases. Tables 4, 5 and 6 give the various aerodynamic coefficients computed for the three cases of flap deflection.

For $\delta = 0^\circ$ and $\delta = 10^\circ$ the stall angle is around 16° whereas for $\delta = 20^\circ$, the predicted stall angle is at around 12° . Another important feature that can be observed is that for all the three flap deflection the characteristic curves are parallel in the linear region. Figures 8(b) and (c) show the variation of C_D with C_L and variation of C_M with angle of attack α .

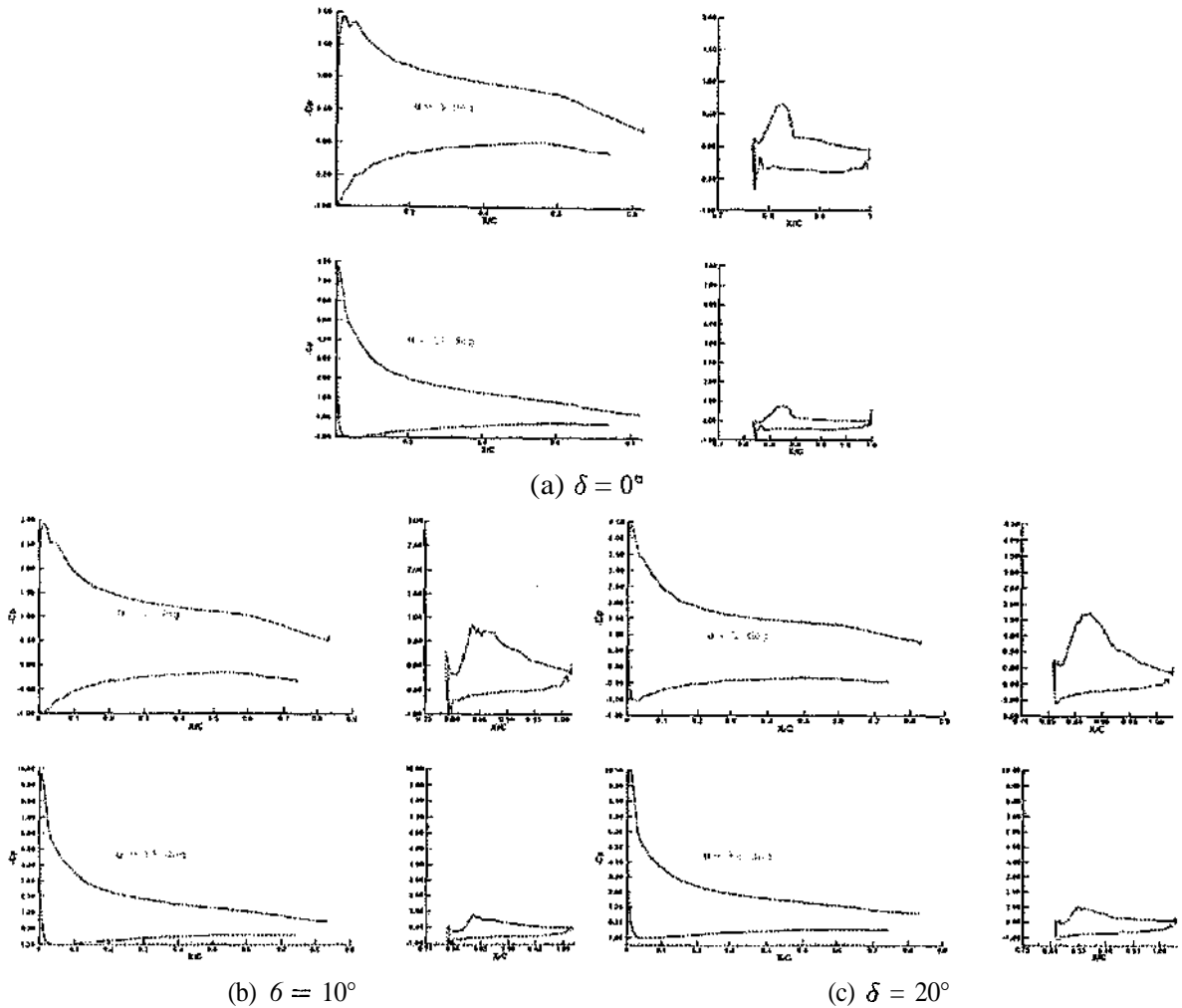


Fig.9: Pressure coefficient on HANSA-3 aerofoil with modified flap: MOO = 0.3, $Re_\infty = 2 \times 10^6$

respectively.

Figures 9(a), (b) and (c) show the computed pressure coefficients for the three cases respectively. For each flap deflection pressure coefficients are shown for $\alpha = 5^\circ$ and $\alpha = 14^\circ$.

Figure 10(a) shows a comparison of the flow pattern for $\delta = 0^\circ$ and $\alpha = 10^\circ$ between the existing and modified configurations with streamlines superimposed on pressure contours. For this case both the configurations show the attached flow on both the aerofoil and the flap. Figure 10(b) shows a similar comparison for $\delta = 20^\circ$ and $\alpha = 10^\circ$. It can be clearly observed that the existing configuration exhibits a large portion of separated region over the flap whereas the modified one shows a very smooth behaviour having fully attached flow throughout with a small cove vortex in the gap close to the trailing edge of the main aerofoil.

Finally Fig.11 shows streamline pattern superim-

posed on pressure contours for post stall cases for the modified aerofoil flap configuration for $\delta = 0^\circ$, 10° and 20° wherein one can see large regions of separated flow with vortex structures on the flow downstream of the trailing edge of the main aerofoil. Cove vortices are also seen for $\delta = 10^\circ$ and $\delta = 20^\circ$ in the gap region.

4 Conclusions

The code JUMBO2D has been validated against experimental results for flow past GA(W)-2 aerofoil with deflected flap. Using the same code an aerofoil-flap configuration has been designed which gives an attached flow up to a moderate angle of attack and flap deflection angle up to 20° for a low speed two-seater trainer aircraft HANSA-3. For better response of the flap, flow should remain attached up to the stall which has been achieved in the present configuration. The present design, compared to the previous [12, 13] one, does not call for any major modification in main airfoil

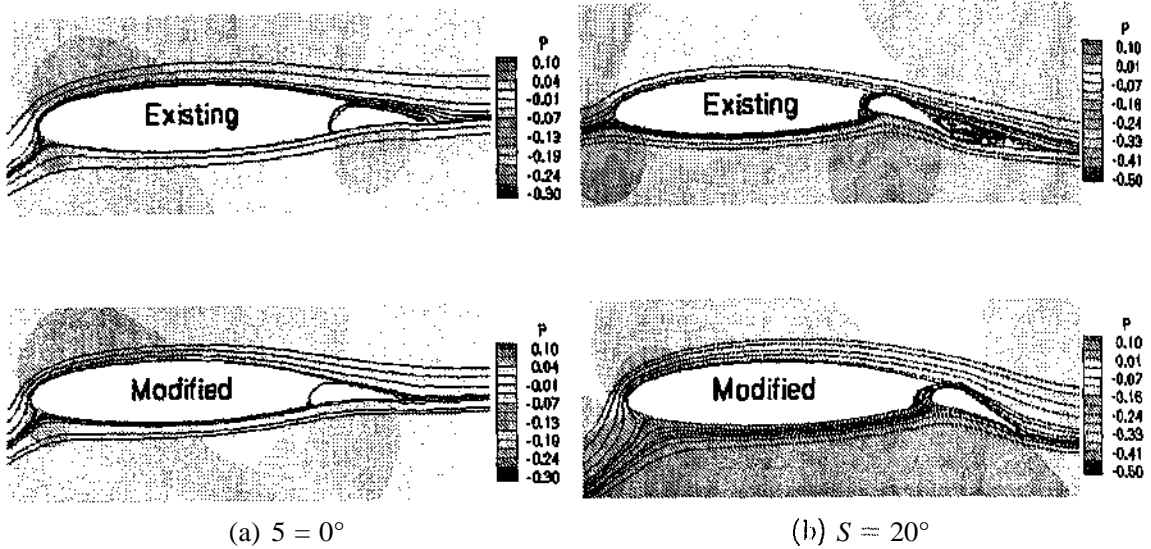
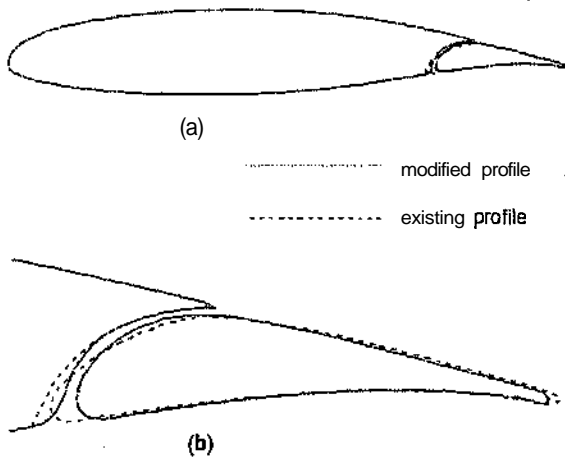


Fig.10: Streamlines and pressure contours of the existing and modified flap Configurations, $M_\infty = 0.3, Re_\infty = 2 \times 10^6, \alpha = 10^\circ$



Point of rotation :

Existing : (0.826,-0.0766) or (1079mm, 100mm)

Modified: (0.830,-0.1200) or (1084mm, -156mm)

Fig.5: Comparison of the existing and the modified profiles of the main aerofoil with flap

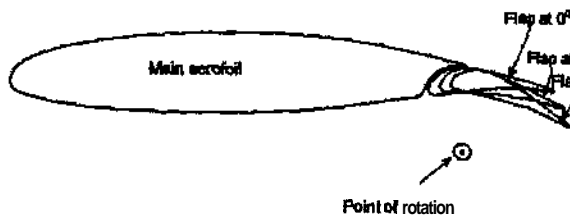


Fig.6: Redesigned aerofoil and flap configuration with three positions of deflected flap

α	C_L	C_D	C_M	C_{Df}
-10.00	-0.763655	0.021806	-0.070700	0.61775E-02
-5.00	-0.145999	0.009574	-0.097184	0.6887GE-02
0.00	0.417103	0.009386	-0.101308	0.71042E-02
5.00	0.991552	0.016391	-0.106025	0.70504E-02
10.00	1.566488	0.031543	-0.113178	0.6821GE-02
12.00	1.799174	0.040790	-0.110758	0.05779E-02
14.00	1.859049	0.048459	-0.087396	0.62216E-02
16.00	1.926502	0.059013	-0.000155	0.5714CE-02
18.00	1.766988	0.009774	-0.027872	0.50454E-02

Table 4: Hansa-flap : Aerodynamic coefficients for different α , $M_\infty = 0.3, S = 0^\circ, Re_\infty = 2 \times 10^6$

α	C_L	C_D	C_M	C_{Df}
-10.00	-0.177145	0.013750	-0.202516	0.66938E-02
-5.00	0.449913	0.010665	-0.225649	0.72952E-02
0.00	1.012599	0.016390	-0.228601	0.63661E-02
5.00	1.493297	0.024983	-0.209516	0.76293E-02
10.00	2.006717	0.042769	-0.198554	0.71264E-02
12.00	2.174249	0.053695	-0.187476	0.67529E-02
14.00	2.280601	0.070074	-0.168963	0.60147E-02
16.00	2.292746	0.096881	-0.146014	0.48992E-02
18.00	1.794785	0.143328	-0.115954	0.39370E-02

Table 5: Hansa-flap : Aerodynamic coefficients for different α , $M_\infty = 0.3, \delta = 10^\circ, Re_\infty = 2 \times 10^6$

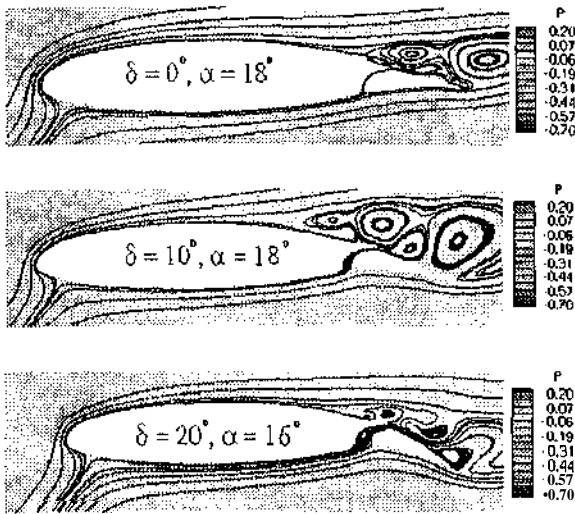


Fig.11: Streamlines and pressure contours of the modified flap configuration just after stall:
 $M_\infty = 0.3, Re_\infty = 2 \times 10^6$

a	C_L	C_D	C_M	C_{Df}
-10.00	0.335244	0.013173	-0.308778	0.70974E-02
-7.00	0.741297	0.011582	-0.332624	0.74518E-02
0.00	1.514660	0.021808	-0.343470	0.76626E-02
2.00	1.724281	0.026761	-0.339476	0.76272E-02
5.00	2.002880	0.035644	-0.337004	0.75095E-02
10.00	2.520789	0.061370	-0.311342	0.68157E-02
12.00	2.032156	0.079123	-0.287179	0.59673E-02
14.00	2.471509	0.115147	-0.234736	0.49327E-02
16.00	2.157746	0.148511	-0.183746	0.40532E-02
18.00	1.861722	0.173776	-0.102385	0.31578E-02

Table G: Hansa-flap : Aerodynamic coefficients for different n , $M_\infty = 0.3, S = 20^\circ, Re_\infty = 2 \times 10^6$

profile. Smooth flow patterns observed in the present study should be of interest to the designers.

Acknowledgement

The authors thank Dr. S. S. Desai, Head, Computational and Theoretical Fluid Dynamics Division, NAL for his keen interest and encouragement for this work. The authors also take this opportunity to thank the authorities of Centre for Civil Aircraft Design and Development (C-CADD(F)) for showing keen interest and for providing the geometrical data of HANSA-3 aerofoil and flap configuration. Contribution of Dr. J. S. Mathur at the initial stage of this work is acknowledged. Many useful discussions the authors had with the colleagues of CTFD division are also gratefully acknowledged.

REFERENCES

- [1] Pointwise Inc., "Gridgen User Manual Version 13", 1998.
- [2] Chakrabartty, S. K., Mathur, J. S. and Dhanalakshmi, K., "Application of advanced CFD codes for aircraft design and development at NAL", Journal of Aerospace Sciences and Technologies (formerly Jour. of Aero. Soc. of India), Vol.55, No.1, pp74-88, February 2003.
- [3] Chakrabartty, S. K., "A finite volume nodal point scheme for solving two dimensional Navier-Stokes equations", Acta Mechanica, Vol. 84, pp.139-153, 1990.
- [4] Chakrabartty, S. K., Dhanalakshmi, K., "Navier-Stokes analysis of Korn aerofoil", Acta Mechanica, Vol. 118, pp. 235-239, 1996.
- [5] Chakrabartty, S. K., Dhanalakshmi, K. and Mathur, J. S., "Navier-Stokes analysis of flow through two-dimensional cascades", Computational Fluid Dynamics Journal, Vol.10, No.2, pp233-241, 2001.
- [6] Baldwin, B. S. and Lomax, H., "Thin layer approximation and algebraic model for separated turbulent flows", AIAA Paper 78-257, 1978.
- [7] Chakrabartty, S. K., Dhanalakshmi, K., "Computation of transonic flows with shock-induced separation using algebraic turbulence models", AIAA Journal, Vol. 33, No. 10, pp. 1979-1981, 1995.
- [8] Chakrabartty, S. K., Dhanalakshmi, K. and Mathur, J. S., "Computation of flow past aerospace vehicles", Current Science, Vol. 77, No. 10, pp 1295-1302, 1999.
- [9] Vimala Dutta and Desai, S. S., "Position of a stall warning system on HANSA-3 prototype-II", NAL Project Document CF-9905, 1999.
- [10] Wentz, W.H., Jr., "Wind tunnel tests of GA(W)-2 airfoil with 20% Aileron, 25% Slotted Flap, 30% Fowler Flap, and 10% Slot-lip Spoiler", Aeronautical Report 7C-2, August 1976.
- [11] Wentz, W.H., Jr., and Fisco, K., "Pressure Distribution for the GA(W)-2 airfoil with 20-percent aileron, 25-percent slotted flap and 30-percent fowler flap", Aeronautical Report 76-3, January 1977.
- [12] Chakrabartty, S. K., Dhanalakshmi, K. and Ramesh, V., "Redesign of HANSA Flap using CFD", NAL Project Document CF 0203 March 2002.
- [13] Chakrabartty, S. K., Dhanalakshmi, K. and Ramesh, V., "Navier-Stokes Analysis and Design of Aerofoil-Flap Configurations for Low Speed Aircraft", Computational Fluid Dynamics Journal, Vol. 11, No.-3, pp 285-289, October 2002.